Polyelectrolyte Adsorption on an Oppositely Charged Spherical Particle. Chain Rigidity Effects

Serge Stoll* and Pierre Chodanowski

Analytical and Biophysical Environmental Chemistry (CABE), Department of Inorganic, Analytical and Applied Chemistry, University of Geneva, Sciences II, 30 quai E. Ansermet, CH-1211 Geneva 4, Switzerland

Received February 19, 2002; Revised Manuscript Received August 23, 2002

ABSTRACT: We used Monte Carlo simulations to study the formation of complexes between a flexible, semiflexible, and rigid polyelectrolyte and an oppositely charged spherical particle. Polyelectrolyte adsorption on a small particle, whose surface curvature effect is expected to limit the amount of adsorbed monomers, was considered. We focused on the effects of the intrinsic polyelectrolyte rigidity and ionic concentration of the solution and investigated the adsorption/desorption limit and conformation of the adsorbed polyelectrolyte. Polyelectrolyte adsorption is controlled by several competing effects such as the electrostatic confinement energy of the chain due to the electrostatic repulsions between the charged monomers, polyelectrolyte intrinsic flexibility, and electrostatic attractive interaction between the polyelectrolyte monomers and the particle. On one hand, rigidity and electrostatic repulsions force the polyelectrolyte to adopt extended conformations and limit the number of monomers that may be attached to the particle. On the other hand, electrostatic attractive interactions between the particle and the polyelectrolyte monomers force the chain to undergo a structural transition and collapse at the particle surface. In particular, by increasing the intrinsic rigidity, we observed a transition from a disordered and strongly bound complex to a situation where the polymer touches the particle over a finite length, while passing by the formation of a solenoid conformation. We found that the critical ionic concentration at which adsorption/desorption is observed is rapidly decreasing with the polyelectrolyte intrinsic rigidity, and the amount of adsorbed monomers has a maximum value for semiflexible chains. Adsorption is thus promoted by decreasing the chain stiffness or decreasing the salt concentration for a given chain length.

Introduction

Because of their fascinating, complex, and important modifications of solutions properties, mixtures of polyelectrolyte chains and comparatively small oppositely charged objects such as colloidal particles, proteins, micelles, vesicules, etc., stimulate a great interest in colloid science.[1−3] Applications in the field of water treatment such as flocculating/water insoluble mixtures, adhesion, food technology, and powder processing are numerous,[4−6] and extension to gene therapy and bioengineering is today under consideration.[7] Also in environmental chemistry, interactions between inorganic colloids and biopolymers are also of great interest since complexation processes are expected to control colloid coagulation and the fate and transport of trace polluants associated with the inorganic colloids.[8,9]

However, the long-range attractive and/or repulsive character of electrostatic interactions, solution chemistry, chemical nature, geometry and concentration of both polyelectrolytes and particles, competitive adsorption, etc., give these solutions very specific properties which are partially understood. Thus, so far, little is known in the rational use of polyelectrolytes with oppositely charged particles. By considering the polyelectrolyte charge fraction and salt concentration, Haronska et al.[10] proposed a theoretical model (based on a self-consistent approach) for the complex formalism of flexible polyelectrolytes and oppositely charged spheres. A particular emphasis on the influence of the finite size of both polyelectrolyte and sphere was considered. The theoretical results were compared with the adsorption of PMA on a cationic micronetwork, and it was demonstrated that the criterion for critical adsorption shows a different behavior for small and large curvature of the sphere. Dobrynin et al.[11] developed a scaling theory of polyelectrolyte adsorption at an oppositely charged surfaces. At low surface charge densities, they predicted two-dimensional adsorbed layers with thickness determined by the balance between electrostatic attraction to the charged surface and chain entropy whereas at high surface charge densities, they expected a 3-dimensional layer with a density profile determined by the balance between electrostatic attraction and short-range monomer−monomer repulsion. The adsorption of weakly charged polyelectrolytes at planar and oppositely charged surfaces was modeled by Linse and Shubin[12,13] using a mean-field lattice theory for flexible polyelectrolytes in solution. They demonstrated that in most cases, as salt concentration is increased, the adsorbed amount is reduced but the thickness of the adsorbed layer is increased. Using a combination of variational procedures and ground-state dominance approximation as well as off-lattice Monte Carlo simulations, Von Goeler, Muthukumar, and Kong[14,15] derived explicit formula for the dependence of adsorption characteristics of polyelectrolytes onto curved surfaces (spheres and cylinders) on temperature, Debye screening length, polyelectrolyte charge density, molecular weight, and curvature. Adsorption was found to be promoted by lowering temperature, chain length, and salt concentration and by increasing the radius and the surface charge density of the sphere. Thermodynamic as well as kinetic factors controlling the stability of colloid/polymer mixtures have been addressed experimentally by Dubin and co-workers[16] by considering interactions between polyelectro-

* To whom correspondence should be addressed.

10.1021/ma020272h CCC: $22.00
Published on Web 11/02/2002

lytes and micelles. Critical conditions for adsorption vs pH and ionic concentration were reported, showing that the required critical surface charge density of the micelles necessary for adsorption was proportional to the inverse Debye screening length κ.

Recently, the overcharging issue or charge inversion has attracted significant attention and debates. Indeed, in some conditions, the adsorption of a charged polymer (or a macroion) on an oppositely charged colloid can induce charge inversion of the colloid. Mateescu et al.[17] have shown that overcharging increases with the diameter of the colloid (continuously or though multiple transitions), until a total collapse of the polyelectrolyte takes place. Nguyen, Grosberg, and Shklovkii[18,19] have investigated complexation for both salt-free and salty solutions and demonstrated that polyelectrolyte winds around the macroion, its turn repealing each other and forming an almost equidistant solenoid. They also demonstrated that adding monovalent salt makes charge inversion stronger, exceeding 100% is some cases. By studing an idealized model for the adsorption of weakly charged polyelectrolyte, Gurovitch and Sens[20] predicted that the connectivity between the charges of the polymer leads to an overcharge of the colloidal particle, which can adsorb a chain of total charge up to 15/6 times its own charge.

The behavior of polyelectrolyte/particle complexes is usually described by considering the ionic concentration of the solution, polyelectrolyte charge linear density, particle charge, and radius. Nonetheless, an essential parameter is the chain flexibility which includes both chain stiffening due to electrostatic monomer−monomer repulsions and stiffness of the underlying chain backbone (intrinsic flexibility). Until now, very few studies have considered the role of the chain intrinsic flexibility in the polyelectrolyte/particle complex formation. Sintes et al.[21] investigated the problem of adsorption of a single semiflexible polymer chain onto a planar, homogeneous surface using Monte Carlo simulations. Adsorption characteristics were studied at different temperatures for chains of various stiffness. They demonstrated that the stiffer chains adsorb more onto the surface and the adsorption takes place at a higher temperature when compared to that of a flexible chain. The effect of copolymer sequence distribution and stiffness on the adsorption−desorption transition temperature was also examined using Monte Carlo by Chidambaram and Dadmun.[22] Netz and Joanny[23,24] recently provided a full complexation phase diagram for a stiff polyelectrolyte in the presence of an oppositely charged sphere. Both the effects of added salt and chain stiffness were taken into account. They demonstrated that for intermediate salt concentration and high sphere charge a strongly bound complex, where the polymer completely wraps around the sphere, is obtained and that the low salt regime is dominated by monomer−monomer repulsions leading to a characteristic hump shape where the polymer partially wraps around the sphere with two polymer arms extended parallel and in opposite directions from the sphere. In the high salt regime, they suggested that the polymer partially wraps the sphere. They also provided an adsorption criterion and then derived the density distribution of the adsorbed polyelectrolyte to calculate the particle radius, below which adsorption does not occur because of curvature effects. Adsorption/desorption limits as well as charge reversal mechanism were investigated, revealing that an increase in the chain stiffness promotes chain desorption. The binding of one semiflexible polyelectrolyte onto an oppositely charged sphere, using parameters appropriate for DNA−histone complexes was studied numerically by Kunze and Netz.[25] They find complete wrapping for intermediate salt concentration, discontinuous dewrapping for high salt concentration, and multiple conformational transition for low salt concentration in agreement with experiments. The wrapped conformations were characterized by four distinct structures with rotational and mirror symmetries. As the complexation free energy was much larger than k_BT, thermally induced dewrapping was neglected in the main part of the phase diagram which was given. Park, Bruinsma, and Gelbart[26] shown that spontaneous overcharging in polyelectrolyte−colloid complexes was accounted for in the Poisson−Boltzmann approximation, and increasing the rigidity of the polyelectrolyte was leading to undercharging of the complex. Mateescu, Jeppesen, and Pincus[17] demonstrated the existence of a "wrapping transition" between a slightly bent conformation of the polyelectrolyte close to the sphere and a conformation where the polyelectrolyte wraps or collapses around the sphere. This "wrapping transition" is expected to be dependent on the salt concentration and sphere diameter.

Monte Carlo simulations have corroborated some experimental and theoretical conclusions. Chain flexibility, linear charge density, and micelle radius were considered by Wallin and Linse[27−29] to investigate the behavior of a polyelectrolyte−micelle complex. They concentrated on free energy calculations to determine the key parameters influencing critical aggregation concentration. Critical aggregation concentration was found to increase with decreasing chain stiffness, linear charge density, and micelle radius. The complexation between a linear flexible polyelectrolyte and several oppositely charged macroions was recently examined by Jonsson and Linse[30,31] with focus on effect of linear charge density, chain length, macroion charge, and chain flexibility. Composition, structure, and thermodynamic properties of the complexes were obtained and the overcharging issue and location of small ions investigated. Owing to the important potential of computer simulations to provide qualitative and quantitative means of understanding the factors that could influence polyelectrolyte/particle interactions, we used a Monte Carlo approach to get insight into the behavior of a flexible, semiflexible, and rigid polyelectrolyte with the presence of an oppositively small charged particle. As the ionic concentration is expected, via screening effects, to play a key role in controlling both chain conformation (via the electrostatic persistence length) and polyelectrolyte/particle interaction energy, we also focused on it. A simple model with a uniformly charged hard sphere to mimic a colloidal particle and a pearl necklace chain consisting of point charges connected to each other is used. Since a Debye−Hückel approach is considered, ions and counterions are implicitely considered. The adsorption/desorption limit which is a key parameter for technical applications of polyelectrolyte/particle mixtures dependence with the ionic concentration and chain intrinsic flexibility is calculated. The polyelectrolyte conformations are analyzed prior to and after adsorption; the polymer interfacial structure is investigated as well as the particle surface coverage and polyelectrolyte adsorbed amount. Snapshots of equili-

brated conformations are also provided to achieve qualitative views of the polymer/particle complexes. Recently we described in detail the complex formation between a charged colloidal particle and an oppositely charged polyelectrolyte.[32,33] The formation of a polyelectrolyte−particle complex was investigated with special attention focused on the effect of the particle size, chain length, and salt concentration on the adsorption/desorption limit, interfacial structure, and overcharging issue.

Model

A pearl necklace model is used to generate off-lattice 3-dimensional chains. They are represented as a succession of N freely jointed hard spheres, and each sphere is considered to be a physical monomer of radius σ_m = 3.57 Å with a negative charge equal to −1 on its center. The fraction of ionized monomers f is set to 1, and the bond length is constant and equal to the Bjerrum[34] length l_B = 7.14 Å.

The particle is represented as an impenetrable, uniformly charged sphere with a radius σ_p equal to 35.7 Å so as to get full insight into particle curvature effects. The particle surface charge is assumed to be concentrated into a point charge located at its center. The central point charge Q of the particle is adjusted to +100 so as to keep a constant surface charge density equal to +100 mC m^{-2}, which is representative of values observed for natural inorganic particles at neutral pH. The solvent is treated as a dielectric medium with a relative dielectric permittivity constant ϵ_r taken as that of water at 298 K, i.e., 78.5. The total energy E_{tot} (k_BT units) for a given conformation is the sum of repulsive electrostatic interactions between monomers and attractive electrostatic interactions between the chain and the particle, E_{el}, and E_{tor}, the chain stiffness or bending energy. Hard-core interactions E_{ev} are also considered to include both monomer and particle excluded volumes.

$$E_{tot} = E_{ev} + E_{el} + E_{tor} \tag{1}$$

Hard-core repulsions between i and j physical units lead to excluded-volume interactions using

$$E_{ev} = \sum_{i<j} u_{EV}(r_{ij}) \tag{2}$$

with

$$u_{ev}(r_{ij}) = 0 \quad \text{when } r_{ij} > \sigma_i + \sigma_j \tag{3}$$

$$u_{ev}(r_{ij}) = \infty \quad \text{when } r_{ij} \le \sigma_i + \sigma_j \tag{4}$$

where σ_i represents the radius of unit i (which can be the monomer or the particle) and r_{ij} the distance between the centers of the two units.

All pairs of charged monomers within the polyelectrolyte interact with each other via a screened Debye−Hückel long-range potential,

$$u_{el}(r_{ij}) = \frac{z_i z_j e^2}{4\pi\epsilon_r\epsilon_0 r_{ij}} \exp(-\kappa r_{ij}) \tag{5}$$

where z_i represents the amount of charge on unit i.

Monomers interact with the particle according to a Verwey−Overbeek potential,

$$u'_{el}(r_{ij}) = \frac{z_i z_j e^2}{4\pi\epsilon_r\epsilon_0 r_{ij}} \frac{\exp[-\kappa(r_{ij} - \sigma_p)]}{1 + \kappa\sigma_p} \tag{6}$$

Free ions are not included explicitly in the simulations, but their overall effects on monomer−monomer and monomer−particle interactions are described via the dependence of the inverse Debye screening length κ^2 [m^{-2}] on the electrolyte concentration according to

$$\kappa^2 = 1000 e^2 N_A \sum_i \frac{z_i^2 C_i}{\epsilon_0\epsilon_r k_B T} \tag{7}$$

It is worth noting here that all pairwise interactions have been calculated without taking into account cutoff distances, and the entropy of counterion release is only captured on a linear level. The intrinsic chain stiffness is adjusted by a square-potential with variable amplitude to vary its strength. This gives the bending energy

$$E_{tor} = \sum_{i=2}^{N} k_{ang}(\alpha_i - \alpha_0)^2 \tag{8}$$

where $\alpha_0 = 180°$ and α_i represents the angle achieved by three consecutive monomers $i-1$, i, and $i+1$. k_{ang} [k_BT/deg^2] defines the strength of the angular potential or chain stiffness.

Monte Carlo simulations were performed according to the Metropolis algorithm in the canonical ensemble. In this method successive "trial" chain configurations are generated to obtain a reasonable sampling of low-energy conformations.[35] To generate new conformations, the monomer positions are randomly modified by specific movements; the end-bond, kink-jump, crankshaft, pivot, and reptation. After each elementary random movement, the Metropolis selection criterion is employed to either select or reject the move. The central monomer of the chain is initially placed at the center of a large three-dimensional spherical box having a radius equal to $2N\sigma_m$, and the particle is randomly placed in the cell. The polyelectrolyte and the oppositely charged particle are then allowed to move. After each calculation step, the coordinates of both the particle and monomers are translated in order to replace the central monomer in the middle of the box. It should be noted that the chain has the possibility to diffuse further away and leave the particule surface during a simulation run (desorption process). After relaxing the initial conformation through 10^6 cycles (equilibration period), chain properties are calculated and recorded every 1000 cycles. Owing to the large number of possible situations with regards to the modifications of both k_{ang} and C_i, the application of this model with regards to processor speeds has currently limited the chain length to 100 monomer units (200 for the isolated chain).

To characterize chain configurations relative to the surface such as the mean-square radius of gyration $\langle R_g^2 \rangle$ and the mean-square end-to-end distance $\langle R_{ee}^2 \rangle$, ensemble averages (denoted by $\langle\ \rangle$) are calculated after the equilibration period. To determine the position of the chain monomers along the coordinate normal to the surface, spherical layers around the surface are defined. The thickness of each layer, excepted the first one, is set to one monomer radius. Because an adjacent layer of one monomer radius in thickness is rarely visited (because of strong excluded-volume effects between the

monomers and the surface), the thickness of the first layer was arbitrarily increased to two monomer radii. To characterize the conformation of the adsorbed chain, the mononer fraction in tails, loops, and trains has been considered. Two parameters, the particle surface coverage θ and the adsorbed amount of polyelectrolyte Γ, are also calculated to characterize the particle surface with regards to the number of monomers in the first layer. Surface coverage is defined as the fraction of the particle surface covered with the monomers which are present in the first layer,

$$\theta = \frac{a_0 N^*}{a_{surf}} \tag{9}$$

where a_0 is the projected area of one monomer, N^* the number of adsorbed monomers lying in the first layer, and a_{surf} the surface of the particle and the adsorbed amount GΓ defined as

$$\Gamma = \theta/\theta_{max} \tag{10}$$

where $\theta_{max} = Na_0/a_{surf}$ is the maximum fraction of particle surface area that can be covered by a fully adsorbed polymer chain. To calculate the isolated polyelectrolyte persistence length L_p, we used the bond-angle correlation function BAC defined by the scalar product between the normalized bond vectors. The persistence length is then defined as the decay contour length of all angular correlations, and the function BAC exhibits an exponential decay such as

$$\mathrm{BAC}(k) \sim \exp\left(-\frac{k}{L_p}\right) \tag{11}$$

where k represents the contour distance along the polyelectrolyte chain and L_p is the sum of the intrinsic part L_0 and electrostatic contribution L_e.

Configurational Properties of Isolated Semiflexible Polyelectrolyte Chains

Equilibrated conformations of isolated semiflexible polyelectrolyte chains (used as initial conformations at the beginning of the calculations) are discussed first vs C_i and k_{ang} for comparison with adsorbed conformations. Electrolyte concentration ranges from $C_i = 0$ ($\kappa^{-1} = \infty$) to $C_i = 1$ M ($\kappa^{-1} = 3$ Å), k_{ang} values are adjusted from 0 to 0.02 k_BT/deg^2, and the chain length is equal to 200 monomers. Table 1 demonstrates that the semiflexible polyelectrolytes exists as extended and SAW configurations which are controlled by both the intensity of the electrostatic repulsions between the monomers and intrinsic stiffness k_{ang}. When $k_{ang} = 0$ k_BT/deg^2, i.e., when fully flexible chains are considered, a decrease in the ionic concentration causes a gradual spreading of the polyelectrolyte dimensions so that rodlike structures are achieved to minimize the electrostatic energy of the chain. Rodlike here does not mean a straight pole but rather a highly oriented object because of the monomer thermal fluctuations causing movements and local chain deformation. According to our model and effect of the monomer excluded volume giving raise to an intrinsic persistence length equal to 15 Å, screening is expected to destroy the local electrostatic stiffening when the electrostatic persistence length L_e becomes smaller than L_0. The self-avoiding walk limit is thus expected to be achieved (by representing from Table 2 the variation of L_e vs κ^{-1}) when κ^{-1} becomes smaller than 2 Å, i.e., when C_i is greater than 2.3 M.

Table 1. Monte Carlo Equilibrated Conformations of Isolated Polyelectrolytes ($N = 200$) as a Function of the Intrinsic Polyelectrolyte Stiffness k_{ang} and Ionic Concentration C_i[a]

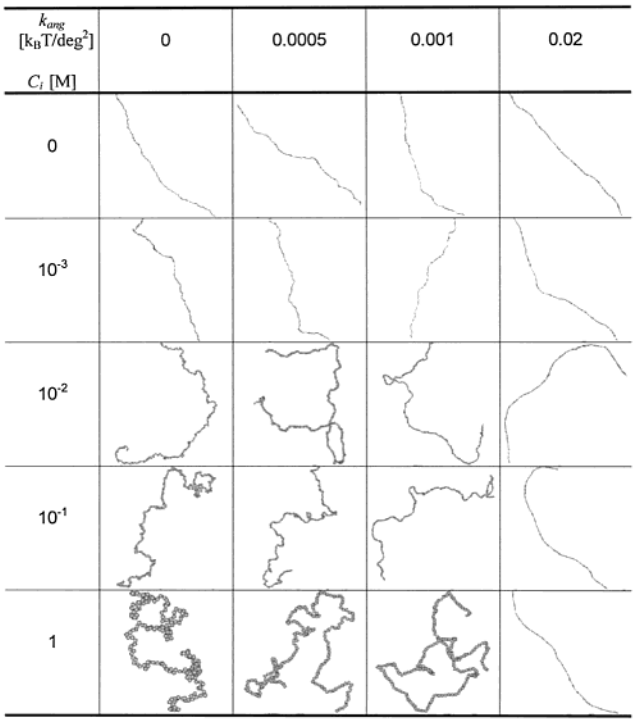

[a] When electrostatic interactions between monomers are screened ($C_i = 1$ M), the increase of the chain stiffness induces the formation of rigid domains which are connected to each other by more flexible regions.

When $C_i = 1$ M, so that the chain stiffness is expected to have predominant effects, a novel picture of chain stretching must be considered. The increase of intrinsic stiffness locally destroys a large amount of chain entropy and results in the formation of rigid domains connected to each other by flexible bonds (see for example Table 1, $C_i = 1$ M and $k_{ang} = 0.001$ k_BT/deg^2). It is important to note that when the salt concentration is infinity (i.e., no electrostatic at all), the chain looks smooth, with no kinks. As shown in Figure 1 where $\langle R_{ee}^2 \rangle$ variations are presented as a function of k_{ang} for different C_i values, electrostatic interactions and intrinsic stiffness influence each other but at different scales. Although long-range electrostatic repulsions have full effects when $C_i = 0$ M, it is still possible to increase the chain dimension through local geometric constraints. It is worth noting that (i) both electrostatic and intrinsic rigidity are required to achieve straight poles and (ii) chain dimensions of screened rigid polyelectrolytes ($C_i = 1$ M and $k_{ang} = 0.02$ k_BT/deg^2) and unscreened flexible polyelectrolyte ($C_i = 0$ M and $k_{ang} = 0$ k_BT/deg^2) are similar.

Polyelectrolyte Adsorption

Adsorption−Desorption Limit. To investigate the complex formation, the charged particle is added to an equilibrated polyelectrolyte chain ($N = 100$) in a large spherical box so that they are close but not in contact to one another. Then the system is let to relax. The polyelectrolyte chain is arbitrarily considered as adsorbed when at least one monomer is in contact with

Table 2. Intrinsic L_0 and Total Persistence Length L_p as a Function of the Chain Stiffness Parameter k_{ang} at Different Ionic Concentration C_i ($N = 100$)

k_{ang} [k_BT/deg^2]	0	0.0005	0.001	0.005	0.01	0.02
$L_{0,CAL}$ [Å]	15	30	52	235	355	910
$L_{p,CAL}$ [Å]						
$C_i = 0$ M/$\kappa^{-1} = \infty$	1814	1664	1651	2171	2713	2724
$C_i = 0.01$ M/$\kappa^{-1} = 30.5$ Å	287	228	177	246	578	1311
$C_i = 0.1$ M/$\kappa^{-1} = 9.6$ Å	73	68	59	220	575	962
$C_i = 1$ M/$\kappa^{-1} = 3.05$ Å	40	31	45	191	568	943

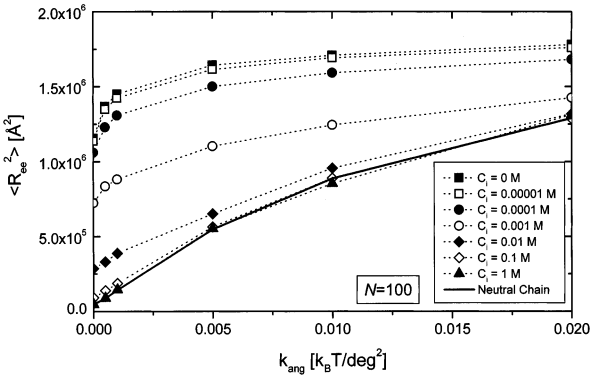

Figure 1. Mean-square end-to-end distance $\langle R_{ee}^2 \rangle$ as a function of the chain intrinsic rigidity k_{ang} at different ionic concentrations C_i. The $\langle R_{ee}^2 \rangle$ variation for a neutral chain is represented by the continuous line. Rigid rods are achieved by both increasing the electrostatic repulsions between the monomers (large-scale effects) and intrinsic stiffness (local effects).

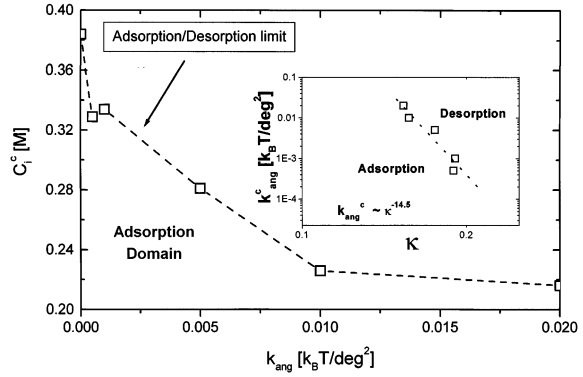

Figure 2. Plot of the critical ionic concentration C_i^C vs k_{ang} at the adsorption/desorption limit. The critical stain stiffness value k_{ang}^c, at which desorption is observed, is shown in the inset vs κ.

Table 3. MC Equilibrated Conformations of Semiflexible Polyelectrolyte/Particle Complexes as a Function of C_i and k_{ang}[a]

C_i [M] / k_{ang} [k_BT/deg^2]	0	0.01	0.1	0.3	1
0	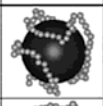	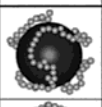	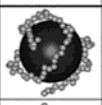	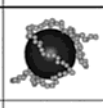	
0.0005	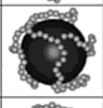	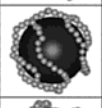			
0.001	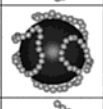	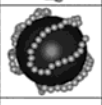	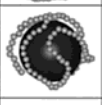		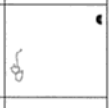
0.005				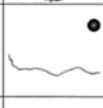	
0.01				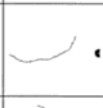	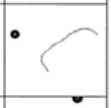
0.02				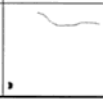	

[a] By increasing the chain stiffness, solenoid conformations are progressively achieved at the particle surface.

the particle during more than 50% of the simulation time. Since the adsorption/desorption transition is sharp, this limit is not sensitive to the criteria we used. Equilibrated configurations as a function of C_i and k_{ang} are presented in Table 3. (Snapshots with extended polyelectrolytes appear smaller than their actual size since they have been reduced in size.) No adsorption is observed when $C_i \geq 1$ M whereas adsorption is always observed when $C_i \leq 0.1$ M. When $C_i = 0.3$ M, Table 3 clearly demonstrates that adsorption is controlled by the value of k_{ang}. Adsorption is promoted by (i) decreasing the chain stiffness (and subsequently the required energy to confine the semiflexible polyelectrolyte at the particle surface) and (ii) decreasing the ionic concentration (increasing thus the electrostatic attractive interactions between the monomer and the particle surface that we consider as the driving force for the adsorption). Because of charge screening in the high salt regime, monomers−particle interactions are not large enough to overcome the polyelectrolyte confinement near the particle.

A quantitative picture of adsorption/desorption is achieved by calculating the critical ionic concentration C_i^C vs k_{ang}, at which the adsorption/desorption process is observed (Figure 2). The adsorption/desorption limit is determined by carefully monitoring the ionic concentration required to satisfy the adsorption/desorption criteria (for a constant k_{ang} value). We found that C_i^C is rapidly decreasing with k_{ang} from 0.38 M to a plateau value at 0.22 M when $k_{ang} > 0.01\ k_BT$/deg^2. In that plateau region, as the polyelectrolyte conformation is similar to that of a rigid rod, the polyelectrolyte is in contact with the particle surface with a few consecutive monomers only, with two polymer arms extended in opposite directions from the particle. We also calculated vs C_i the critical chain stiffness k_{ang}^c at which adsorption/desorption is observed (inset of Figure 2). We found that $k_{ang}^c \sim \kappa^{-\delta}$ (with $\delta = 14.5$), revealing that the increase of chain stiffness rapidly promotes chain desorption on curved surfaces.

Polyelectrolyte Conformation at the Particle Surface. To get an insight into the conformational change due to adsorption, we calculated the mean-square radius of gyration $\langle R_g^2 \rangle$ (Figure 3) as a function of C_i and for different values of k_{ang}. A nonmonotonic behavior of $\langle R_g^2 \rangle$ is observed and results from the complex interplay of attractive particle−monomer, repulsive monomer−monomer interactions at the particle

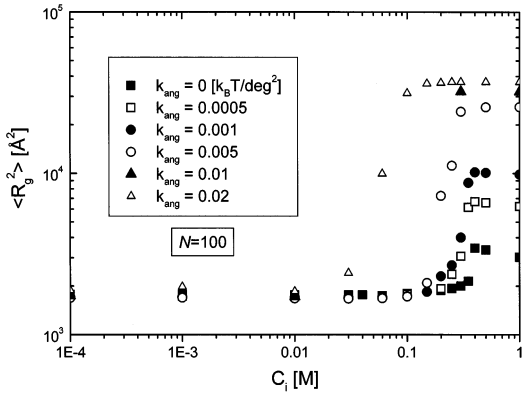

Figure 3. Mean-square radius of gyration $\langle R_g^2 \rangle$ of the polyelectrolyte ($N = 100$) as a function of C_i at different k_{ang} values.

surface, and chain intrinsic flexibility. When $C_i \leq 0.01$ M, because of the strong monomer−particle interactions, the polyelectrolyte completely wraps the particle and chain dimensions do not exhibit a strong dependence with k_{ang}. However, the monomer distribution at the particle surface is largely controlled by the value of k_{ang}. When the chain flexibility is important ($k_{ang} \leq 0.001 k_BT$/deg^2), "tennis ball" conformations are achieved whereas when rigid chains are considered ($k_{ang} > 0.001 k_BT$/deg^2), the intrinsic flexibility forces the polyelectrolyte to adopt solenoid conformations as those predicted by the analytical model of Nguyen and Shkloskii.[19] According to the contour chain length and particle size ratio we investigated, the solenoid achieves approximately three turns ($N\sigma_m/\pi\sigma_p$) around the particle. Both the strong electrostatic repulsions between the neighboring turns and intrinsic chain rigidity keep the turns parallel to each other and a constant distance between them. It is worth noting that the polymer ends are not adsorbed at the particle surface in all cases.

When $C_i > 0.01$ M, the increase of $\langle R_g^2 \rangle$ is promoted via the formation of loops and tails and/or chain desorption. Large changes in the chain dimensions are now observed with increasing the chain stiffness. As long as $k_{ang} \leq 0.001 k_BT$/deg^2, loops and tail are promoted (Table 2; $C_i = 0.3$ M and $k_{ang} = 0.0005\ k_BT$/deg^2), resulting in an increase of the thickness of the adsorption layer. When $k_{ang} \geq 0.005\ k_BT$/deg^2, and with increasing C_i, the polyelectrolyte starts to leave the surface by winding off. Extended tails in solution are formed concomitantly with a decrease in the number of turns of the solenoid and monomers in trains (Table 3; $C_i = 0.1$ M and $k_{ang} = 0.01\ k_BT$/deg^2). By increasing further the ionic concentration or chain intrinsic flexibility, the polyelectrolyte becomes tangent to the particle surface with dimensions close to its free unperturbed dimensions.

Interfacial Region. The number of monomers in trains, loops, and tails as a function of k_{ang} and C_i is presented in Figure 4a−c to get a quantitative insight into the structure of the interfacial region. The monomer fraction in trains has a maximum value when $k_{ang} = 0.005\ k_BT$/deg^2, i.e., when semiflexible chains are considered. Below that value, i.e., when flexible chains are considered, the solenoid conformation is lost and monomers are moving from the first layer to the others to form loops. Above that value, when rigid chains are considered, most of the monomer entropy is lost and ordered solenoid conformations are obtained. By decreasing the attractive monomer−particle interactions, rigid chains desorb to form tails.

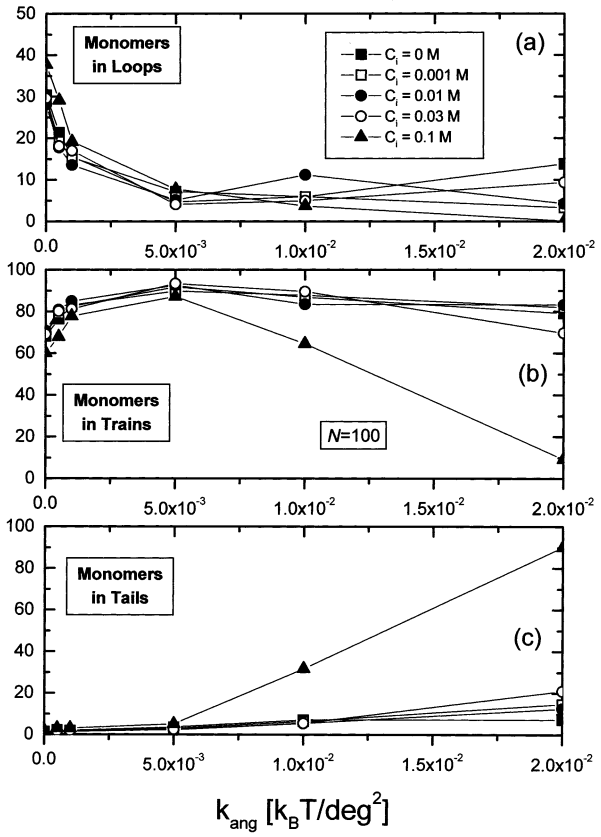

Figure 4. Number of monomers in trains, loops, and tails vs k_{ang} at various ionic concentration values ($N = 100$). Monomers in loops are promoted by decreasing the chain rigidity whereas monomers in trains exhibits a maximum value for semiflexible chains (i.e., when $k_{ang} = 0.005\ k_BT$/deg^2).

Competition between the attractive electrostatic energy and the increase in the torsional energy to control the final complex structure is well illustrated when $C_i = 0.1$ M. By increasing k_{ang}, we obtain a transition from a disordered and strongly bound complex to a situation where the polymer touches the particle over a finite length, while passing by the formation of a solenoid structure. Complexes exhibit a significant monomer loop fraction only when $k_{ang} < 0.001\ k_BT$/deg^2. In the other cases, the fraction of monomers in train decreases while that of the tails increases, monomers being transferred to tails but not to loops. The amount of chain adsorption Γ which is commonly used experimentally to derive adsorption isotherms is presented in Figure 5. Γ is decreasing with increasing the ionic concentration because of monomer desorption. On the other hand, the amount of monomer adsorption has a maximum value when $k_{ang} = 0.005\ k_BT$/deg^2 (i.e., for semiflexible chains) according to the formation of a solenoid without parts extending in the solution. Because of the displacement of the adsorption/desorption limit with k_{ang}, curves cross each other.

Summary and Conclusions

In the present paper, MC simulations have been used to investigate the behavior of a flexible, semiflexible, and rigid polyelectrolyte in the presence of an oppositely charged colloidal particle. The influence of polyelectrolyte intrinsic stiffness and ionic concentration on the adsorption/desorption limit, polyelectrolyte conformation, and monomer distribution on the particle surface was presented. It is shown that computer simulations

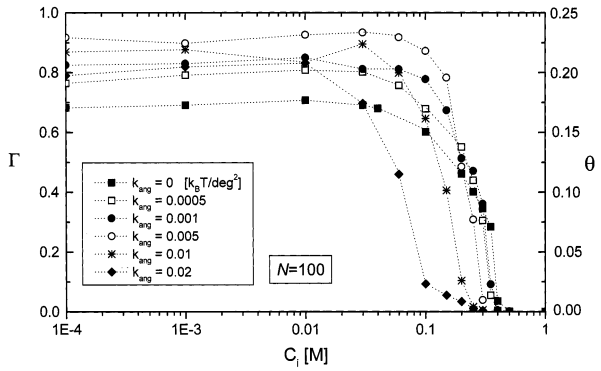

Figure 5. Adsorbed amount Γ and surface coverage θ of the polyelectrolyte and particle respectively vs C_i for different k_{ang} values. Γ reaches a maximum value for the semiflexible chain $k_{ang} = 0.005\ k_BT/\text{deg}^2$ (and with decreasing C_i). Above that value both chain rigidity (by forcing the chain to be extended in solution) and flexibility (monomers are transferred to loops) limit the amount of adsorbed monomers in the first adsorption layer.

can isolate in good agreement the molecular factors that control the polyelectrolyte interfacial behavior and, thus, can help addressing the optimization of colloid−polymer mixtures. Chain stiffness modify the conformation of isolated and adsorbed chains by locally destroying a large amount of monomer entropy. As a result, chain stiffness influences the (i) amount of adsorbed monomers, (ii) monomer distribution at the particle surface, and (iii) adsorption−desorption limit. The amount of adsorbed monomers has a maximun value for the semiflexible chains in the low salt concentration regime. In such conditions, the polyelectrolyte is strongly adsorbed at the particle surface as a solenoid, and the confinement energy does not contribute to the formation of tails in solution. When the chain intrinsic stiffness is small, tennis ball like conformations are achieved. At the opposite, when rigid chains are considered, the polyelectrolyte becomes tangent to the particle. Hence, adsorption is promoted by decreasing the chain stiffness or decreasing the salt concentration for a given chain length.

The simulations reported here are a preliminary step toward a more precise modeling of the problem to understand the behavior of colloid/polymer mixtures. A simple model involving one chain interacting with one particle has been described, but it can be extended to more concentrated systems involving several chains (and/or colloidal particles) as well as polydisperse systems to get insight into complex polymer/particle mixtures and flocculation/stabilization processes. We are currently extending our investigations to investigate the effect of chain linear charge density.

Acknowledgment. The authors express their thanks to B. Shklovslii, T. T. Nguyen, and M. Brynda for their encouragement and stimulating discussions. We gratefully acknowledge the financial support received from the following sources: Swiss National Research Projects 2000-037589.93/1 and 2000-043568.95/1, Commission Suisse pour la Technologie et l'Innovation (CTI), Project Top Nano 21 5950.1, and BASF Corporation.

References and Notes

(1) Barrat, J. L.; Joanny, J. F. In *Advances in Chemical Physics*; Prigogine, I., Rice, S. A., Eds.; Wiley & Sons: New York, 1996; Vol. XCIV.
(2) Xia, J.; Dubin, P. L. Protein-Polyelectrolyte Complexes. In *Macromolecular Complexes in Chemistry and Biology*; Dubin, P., Bock., D., Eds.; Springer-Verlag: Berlin, 1994; p 247.
(3) Muthukumar, M. *J. Chem. Phys.* **1987**, *86*, 7230.
(4) Napper, D. H. In *Polymeric Stabilization of Colloidal Dispersions*; Academic: New York, 1983.
(5) Hara, M. In *Polyelectrolytes: Sciences and Technology*; Dekker: New York, 1993.
(6) Finch, C. A. In *Industrial Water Soluble Polymers*; The Royal Society of Chemistry: Cambridge, 1996.
(7) Rädler, J. O.; Koltover, I.; Salditt, T.; Safinya, C. R. *Science* **1997**, *275*, 810.
(8) Buffle, J.; Wilkinson, K. J.; Stoll, S.; Filella, M.; Zhang, J. *Environ. Sci. Technol.* **1998**, *32*, 2887.
(9) Vermeer, A. W. P.; Leermakers, F.; Koopal, L. *Langmuir* **1997**, *13*, 4413.
(10) Haronska, P.; Vilgis, T. A.; Grottenmüller, R.; Schmidt, M. *Macromol. Theory Simul.* **1998**, *7*, 241.
(11) Dobrynin, A. V.; Deshkovski, A.; Rubinstein, M. *Macromolecules* **2001**, *34*, 3421.
(12) Linse, P. *Macromolecules* **1996**, *29*, 326.
(13) Shubin, V.; Linse, P. *Macromolecules* **1997**, *30*, 5944.
(14) von Goeler, F.; Muthukumar, M. *J. Chem. Phys.* **1994**, *100*, 7796.
(15) Kong, C. Y.; Muthukumar, M. *J. Chem. Phys.* **1998**, *109*, 1522.
(16) Feng, X. H.; Dubin, P. L.; Zhang, H. W.; Kirton, G. F.; Bahadur, P.; Parotte, J. *Macromolecules* **2001**, *34*, 6373.
(17) Mateescu, E. M.; Jeppesen, C.; Pincus, P. *Europhys. Lett.* **1999**, *46*, 493.
(18) Nguyen, T. T.; Grosberg, Y.; Shklovskii, B. I. *J. Chem. Phys.* **2000**, *113*, 1110.
(19) Nguyen, T. T.; Shklovskii, B. I. *Physica A* **2001**, *293*, 324.
(20) Gurovitch, E.; Sens, P. *Phys. Rev. Lett.* **1999**, *82*, 339. Golestanian, R. *Phys. Rev. Lett.* **1999**, *83*, 2473. Sens, P. *Phys. Rev. Lett.* **1999**, *83*, 2474.
(21) Sintes, T.; Sumithra, K.; Straube, E. *Macromolecules* **2001**, *34*, 1352.
(22) Chidambaram, S.; Dadmun, M. D. *Comput. Theor. Polym. Sci.* **1999**, *9*, 47.
(23) Netz, R. R.; Joanny, J. F. *Macromolecules* **1998**, *31*, 5123.
(24) Netz, R. R.; Joanny, J. F. *Macromolecules* **1999**, *32*, 9026.
(25) Kunze, K. K.; Netz, R. R. *Phys. Rev. Lett.* **2000**, *85*, 4392.
(26) Park, S. Y.; Bruinsma, R. F.; Gelbart, W. M. *Europhys. Lett.* **1999**, *46*, 454.
(27) Wallin, T.; Linse, P. *Langmuir* **1996**, *12*, 305.
(28) Wallin, T.; Linse, P. *J. Phys. Chem.* **1996**, *100*, 17873.
(29) Wallin, T.; Linse, P. *J. Phys. Chem. B* **1997**, *101*, 5506.
(30) Jonsson, M.; Linse, P. *J. Chem. Phys.* **2001**, *115*, 3406.
(31) Jonsson, M.; Linse, P. *J. Chem. Phys.* **2001**, *115*, 10975.
(32) Chodanowski, P.; Stoll, S. *J. Chem. Phys.* **2001**, *115*, 4951.
(33) Chodanowski, P.; Stoll, S. *Macromolecules* **2001**, *34*, 2320.
(34) Manning, G. S. *J. Chem. Phys.* **1969**, *51*, 924.
(35) Chodanowski, P.; Stoll, S. *J. Chem. Phys.* **1999**, *111*, 6069.

MA020272H